AN APPROACH TO NUMERICAL EXPERIMENTS FOR ARBITRARY INLET CONDITIONS IN 3D COMPRESSIBLE VISCOUS CASCADE FLOWS

Teruo MIYAZAKI

Department of Mechanical Engineering, Kokushikan University,

4-28-1, Setagaya-ku, Setagaya, Tokyo 154. Japan

For the numerical analysis of the arbitrary non-uniform and unsteady inlet conditions inherent in the rotor flowfields the present method is based on the unsteady three-dimensional compressible Navier-Stokes solver by the pseudo-analytic function theory with the integral operator. The function theory for the initial boundary value problem allows to assign the control surface to any locations in the flowfield. Through the reference points on the control surface, which can stand for any arbitrary aerothermodynamic values, the arbitrary inlet conditions can be introduced. Also the current analysis uses the three different kinds of computation surfaces, which can manage any deflections of their contours. A numerical example was given to demonstrate an important role of the unsteadiness detected at the inlet, which often assumed as negligible, in the turbomachine performance.

Introduction

Usually the flow the turbomachine engine receives from the inlet is non-uniform and unsteady either radially or azimuthally. The proper estimation of the effect of the non-uniformities and unsteadiness on the flow behavior becomes one of the most keenly interested and troublesome problems for the improvement of the performance. Even in a perfectly axi-symmetric inlet there also would be regions of low stagnation pressure near the outer walls. Also these non-uniformities accompanying with unsteadiness lower the stall margin of the fan or compressor and produce stronger secondary flows. Rather difficult phenomena such as inlet distortions, turbulent intakes, multi-row machine problems and, so on, are governed by the completely unstesdy circumstances. The distorted inlet flows, for example, have variations in stagnation pressure and temperature both radially and azimuthally. The prediction of the inlet-engine interaction, therefore, requires the details of the flow in place. However, only approximate experimental techniques, through inserting so-called distortion screens, have been used for the estimation of the interaction. As is well-known, such steady-state distortion testing is not always sufficient because that the strong unsteadiness governing the flow may under- or overestimate the stall margin. Moreover, it may give the wrong informations on the secondary flow phenomena observed in the blade passages.

The current analysis is motivated to present the method which can evaluate the non-uniformity and unsteadiness detected in the inlet flows mentioned. The method is based on the unsteady three-dimensional compressible Navier-Stokes solver using the pseudo-analytic function theory with the integral operator[1), (2)]. The solver uses the three different kinds of computation surfaces, blade-to-blade, meridional and cross-sectional ones those allow any deflections of their contours and can be located anywhere in the flowfield. The arbitrary inlet or upstream condition is evaluated on the control surface and, then introduced through the reference points with the known aerothermodynamic values assigned on the surface. Also the iteration is used in the method. The method[1), 2)] with the supplementary discussion on the reference points can predict the flowfields with the respectively given inlet conditions. The method has som eremarkable characteristics. The envelopes contacting with both blade ends are the cross-sectional surfaces and the blade wall

themselves are the meridional ones. Moreover, the fact that the function theory allows the conventional conformal transformations of the given domains, makes the present code applicable to the arbitrary flowfields. Also the body-fitted coordinates are used. Naturally there are no mesh generation techniques nor complicated selection methods of the coordinates. Owing to the superposability of the solution in the iterative process[3], Duhamel's method can be introduced and it can afford a time-saving, reliable and stable computation even for the non-uniform and unsteady inlet cases. The code requires only moderate size of memory and CPU time consumption of a standard type of the computer systems. The obtained numerical example demonstrated an important role of the unsteadiness detected at the inlet of the axial transonic rotor, which usually assumed as negligible in the experimental studies.

Governing Equations

The continual continuability of the solutions after the pseudo-analytic function theory[4] allows the segmentation of the flowfield even for the unsteady three-dimensional compressible viscous cascade flow with the arbitrary inlet condition[1),(2)]. The governing equations in the blade relative frame for the segmented flowfield between two control surfaces are the continuity equation, the momentum one and the aerothermodynamic relations[1),(2)]. For the relations the energy equation and so on, according to the respectively given physical conditions are introduced. The boundary conditions, at the same time, should be physically and adequately defined. The governing equations are as follows. The continuity equation is

$$\frac{\partial \rho}{\partial t}+\vec{\nabla}(\rho \vec{W})=0 \tag{1}$$

and the momentum equation

$$\begin{aligned}\frac{\partial \vec{W}}{\partial t}&-\vec{W}\times(\vec{\nabla}\times\vec{W})+2\omega\times\vec{W}\\&=\frac{\partial \vec{W}}{\partial t}-\vec{W}\times(\vec{\nabla}\times\vec{V})\\&=-\vec{\nabla} I+T\vec{\nabla} s+\frac{1}{3}\frac{\mu}{\rho}\vec{\nabla}(\mathrm{div}\vec{W})\\&\quad+\frac{\mu}{\rho}\nabla^2\vec{W}\end{aligned} \tag{2}$$

Where W, V, ρ, μ, ω, I, T and s are the relative velocity, absolute velocity, density, viscosity, angular velocity of blades, rothalpy, temperature and entropy per unit mass, respectively. Using the cylindrical coordinates (x, ϕ, r) and the corresponding velocity components (W_x, W_ϕ, W_r), equations (1) and (2) are rewritten as follows.

$$\begin{aligned}&\frac{\partial \log\rho}{\partial t}+\frac{\partial W_x}{\partial x}+\frac{1}{r}\frac{\partial W_\phi}{\partial \phi}+\frac{\partial W_r}{\partial r}+\frac{W_r}{r}\\&\quad+W_x\frac{\partial \log\rho}{\partial x}+W_\phi\frac{\partial \log\rho}{r\,\partial\phi}+W_r\frac{\partial \log\rho}{\partial r}=0\end{aligned} \tag{3}$$

$$\begin{aligned}&\frac{\partial W_x}{\partial t}+W_\phi\left(\frac{1}{r}\frac{\partial W_x}{\partial \phi}-\frac{\partial W_\phi}{\partial x}\right)\\&\quad-W_r\left(\frac{\partial W_r}{\partial x}-\frac{\partial W_x}{\partial r}\right)\\&=-\frac{\partial I}{\partial x}+T\frac{\partial s}{\partial x}+\frac{1}{3}\frac{\mu}{\rho}\frac{\partial \Delta}{\partial x}+\frac{\mu}{\rho}\nabla^2 W_x\end{aligned} \tag{4}$$

$$\begin{aligned}&\frac{\partial W_\phi}{\partial t}-W_x\left(\frac{1}{r}\frac{\partial W_x}{\partial \phi}-\frac{\partial W_\phi}{\partial x}\right)\\&\quad+W_r\left(\frac{\partial W_\phi}{\partial r}-\frac{1}{r}\frac{\partial W_r}{\partial \phi}\right)+\frac{W_r W_\phi}{r}+2\omega W_r\\&=-\frac{1}{r}\frac{\partial I}{\partial \phi}+\frac{T}{r}\frac{\partial s}{\partial \phi}+\frac{1}{3}\frac{\mu}{\rho}\frac{1}{r}\frac{\partial \Delta}{\partial \phi}\\&\quad+\frac{\mu}{\rho}\left(\nabla^2 W_\phi+\frac{2}{r^2}\frac{\partial W_r}{\partial \phi}-\frac{W_\phi}{r^2}\right)\end{aligned} \tag{5}$$

$$\begin{aligned}&\frac{\partial W_r}{\partial t}-W_\phi\left(\frac{\partial W_\phi}{\partial r}-\frac{1}{r}\frac{\partial W_r}{\partial \phi}\right)\\&\quad+W_x\left(\frac{\partial W_x}{\partial x}-\frac{\partial W_r}{\partial r}\right)-\frac{W_\phi^2}{r}-2\omega W_\phi\\&=-\frac{\partial I}{\partial r}+T\frac{\partial s}{\partial r}+\frac{1}{3}\frac{\mu}{\rho}\frac{\partial \Delta}{\partial r}\\&\quad+\frac{\mu}{\rho}\left(\nabla^2 W_r-\frac{W_r}{r^2}-\frac{2}{r^2}\frac{\partial W_\phi}{\partial \phi}\right)\end{aligned} \tag{6}$$

where

$$\nabla^2=\frac{\partial^2}{\partial x^2}+\frac{1}{r^2}\frac{\partial^2}{\partial \phi^2}+\frac{1}{r}\frac{\partial}{\partial r}+\frac{\partial^2}{\partial r^2}$$

and

$$\Delta=\frac{\partial W_x}{\partial x}+\frac{1}{r}\frac{\partial W_\theta}{\partial \phi}+\frac{\partial W_r}{\partial r}+\frac{W_r}{r}$$

On the solid boundaries relatively at rest and on the locations with velocity distributions of zero, the momentum equations are reduced as follows.

$$\nabla^2 W_x=\frac{\rho}{\mu}\left(\frac{\partial I}{\partial x}-T\frac{\partial s}{\partial x}\right)-\frac{1}{3}\frac{\partial \Delta}{\partial x} \quad (7)$$

$$\nabla^2 W_\phi+\frac{2}{r^2}\frac{\partial W_r}{\partial \phi}=\frac{\rho}{\mu}\left(\frac{1}{r}\frac{\partial I}{\partial \phi}-\frac{T}{r}\frac{\partial s}{\partial \phi}\right)-\frac{1}{3}\frac{1}{r}\frac{\partial \Delta}{\partial \phi} \quad (8)$$

$$\nabla^2 W_r-\frac{2}{r^2}\frac{\partial W_\phi}{\partial \phi}=\frac{\rho}{\mu}\left(\frac{\partial I}{\partial r}-T\frac{\partial s}{\partial r}\right)-\frac{1}{3}\frac{\partial \Delta}{\partial r} \quad (9)$$

The additional aerothermodynamic relations as mentioned above are omitted here. The solutions for the equations hitherto mentioned are common to axial-, radial- and mixed-flow types of turbomachines. Therefore, the discussions hereafter, refer only for the axial-flow type.

Solutions for Two different Types of Equations

The governing equations for the initial boundary value problem are solved, using the pseudo-analytic function theory[1),(2)]. The boundary conditions are assigned to the control surface through the reference points. The continuity and the momentum equations are reduced to the simultaneous fundamental differential equations of the complex velocities w_n (n=1,2,3) defined on the respective blade-to-blade, meridional and cross-sectional computation surfaces. The velocities on the respective computation surfaces are calculated through the iteration between the two equations. Pararell with the velocities, the other aerothermodynamic parameters of the flow included in the variable coefficients in the above equations are renewed. The equations in the iterative process[1),(2)] are written as follows.

The first type of equation is such that:

$$\left[\frac{\partial w_n(z_n,\zeta_n,t)}{\partial \zeta_n}\right]_{N+1}=[A_{n,1}(z_n,\zeta_n,t)]_N\,[w_n]_N+[B_{n,1}(z_n,\zeta_n,t)]_N\,\overline{[w_n]}_N+[C_{n,1}(z_n,\zeta_n,t)]_N \quad (10)$$

The second type of equation is such that:

$$M\left[w_n^2\right]+L\left[\frac{\partial w_n^2}{\partial t}\right]=0 \quad (11)$$

where

$$M\left[w_n^2\right]=\frac{\partial w_n^2}{\partial \zeta_n^1}+A_{n,2}^2 w_n^2+B_{n,2}^2\overline{w_n^2}$$

and

$$L\left[\frac{\partial w_n^2}{\partial t}\right]=E_n^2\frac{\partial w_n^2}{\partial t}$$

Here the aerothemodynamic parameters along with the complex velocities at the reference points on the control surface are given or known. The pseudo-analytic function theory[4)] yields the solutions with the integral representations for the respective two types of equations as follows[1),(2)].

$$\begin{aligned}\frac{\alpha}{2}[\dot{W}_n^1(z_n,\zeta_n;t_j)]_{N+1}&=\frac{\alpha}{2}[W_{n,i}(z_n;t_j)]_N+\frac{\alpha}{2}[\Phi_n(z_n,\zeta_n;t_j)]_N\\&-\frac{1}{2\pi i}\oint_{G_n}\frac{[\Phi_n(z'_n,\zeta'_n;t_j)]_N}{z'_n-z_n}*\\&*[1-R_n(z'_n,\zeta'_n,z_{n,1},\cdots,z_{n,m(n)})]\,dz'_n\end{aligned} \quad (12)$$

$$\frac{\alpha}{2}w_n^2(z_n,\zeta_n,t) = -\frac{1}{4\pi i}\int_0^t d\tau \left\{ \int_{G_n} w_n^2(z_n',\zeta_n',\tau)\Omega^{(1)}(z_n,\zeta_n,t;z_n',\zeta_n',\tau)\,dz_n' - \int_{G_n} \overline{w_n^2(z_n',\zeta_n',\tau)}\Omega^{(2)}(z_n,\zeta_n,t;z_n',\zeta_n',\tau)\,d\zeta_n' \right\} \quad (13)$$

where the term for the reference points is

$$R_n = \sum_{k=1}^{m(n)} \frac{P_n}{Q_n} \quad (14)$$

with

$$P_n = (z_n' - z_{n,1})\cdots(z_n' - z_{n,k-1}) * (z_n' - z_{n,k+1})\cdots(z_n' - z_{n,m(n)})$$

and

$$Q_n = (z_{n,k} - z_{n,1})\cdots(z_{n,k} - z_{n,k-1}) * (z_{n,k} - z_{n,k+1})\cdots(z_{n,k} - z_{n,m(n)})$$

Owing to the superposability of the respective solutions under the iterative process[3], the Duhamel's method can be introduced[1],[2]. The method contributes for the time-saving computation. Applying the current method to the segmented flowfields one by one, the solutions for the unsteady three-dimensional compressible viscous flows with the arbitrary inlet conditions can be found eventually.

Numerical Methods

The convergence of the solution by the present method for the flows with the complicated boundary conditions such as the inlet distortion, the turbulent intakes, and so on, is assured theoretically[1],[2]. In the computation the arbitralily given inlet conditions are attained through the iterative scheme, approaching from the simplified conditions to the given ones together with the adequately selected control surface. The solutions of (12) and (13) at the respective computational stages are simultaneously obtained. Additional descriptions of the total scheme for the numerical method and the computation paths are given now.

The Computational Scheme. For the leaned blade row and others, if necessary, the conventional transformations of the coordinates can be applyed, prior to the computation. The present

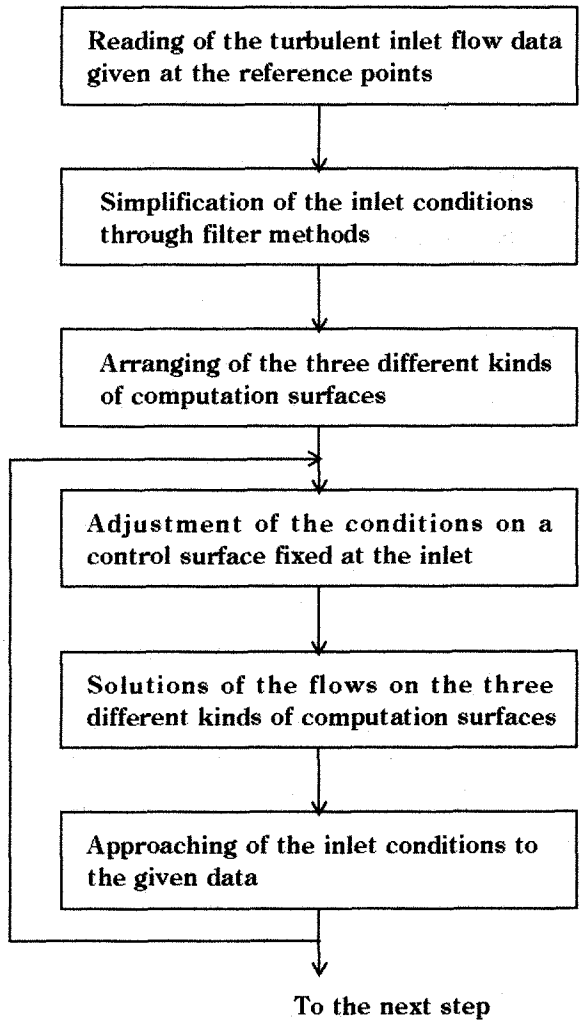

Fig. 1 Turbulent inlet condition

computational schemes for the inlet distortion, for the turbulent intakes, for the multi-row machine, and so on, are similar. Here the scheme for the flow with the turbulent inlet condition, as an example, is shown in Fig. 1.

In the first step, the condition is numerical ly given on the control surface arranged at the inlet. To the reference points the arbitrarily given values are assigned, using the integral operators. In the second step, the given condition is simplified through some filter methods, for example, to assure the stability of the convergence in the iterative computation. In the third step, the three different kinds of computation surfaces are selected to represent the flow phenomena to be discussed. Those surfaces may be rearranged, according to the stages of the iteration. Then the iteration starts, adjusting the values on the control surface in order to approach to the given data and obtaining the solutions on the different kinds of the surfaces. The convergences of the respective numerical solutions are also assured by the pseudo-analytic function theory[1], [2]

The Computation Surfaces. Using the computation surfaces, the scheme can be detailed. Fig. 2 shows the procedure to approach to the given inlet conditions to be aimed on the control surface which placed ahead of the blade row. The assumed inlet conditions for the respective blade-to-blade computations are improved with the iteration process. The aimed inlet conditions at the second and the last stages are numerically represented through the reference points. The segmentation of the flowfield is introduced in the respective computations as shown in Fig. 3. In the segmented flowfield the control surfaces are disposed from the upstream to the downstream and vice versa. At the last stages of the respective computations the segmented flowfields are rearranged and the computation paths are put together as shown in Fig. 4. The figure stands for the meridional computation paths on a blade surface.

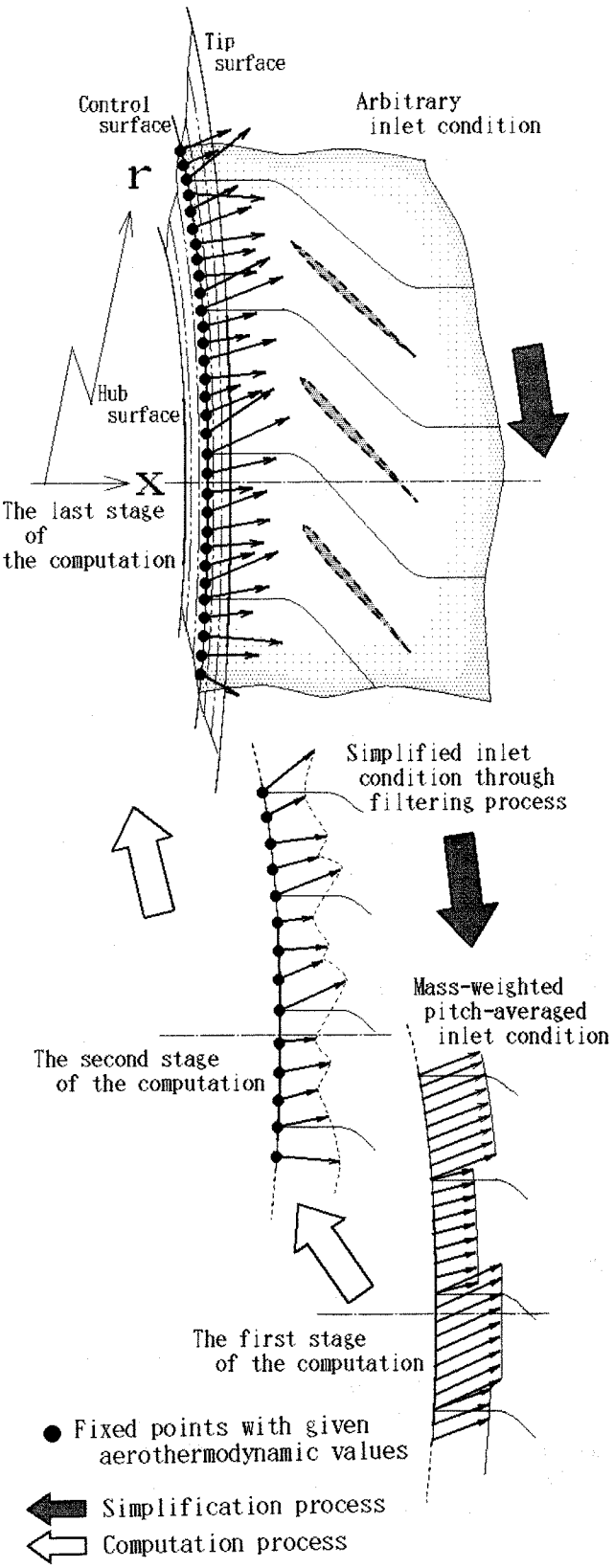

Fig. 2 Arrangement and improvement of inlet conditions

Numerical Example

A numerical example was shown to stress on the important roles of the unsteadiness and non-uniformity detected at the inlet, those were usually assumed as negligible in the experimental studies. As the first approximation of the

iteration the present numerical example employed the obtained results[1] for the axial transonic flow through the 23 bladed overhung rotor without inlet guide vanes installed in MIT Blow Down Facilities[5]. The experimentally supposed tip relative Mach number was 1.30. In the experimental study radially constant stagnation temperature rise, uniform inlet conditions and the shockless through flow were expected. However, the negligible order of deviations in the inlet conditions were observed. In the computation of the results[1], reflecting the experimental circumstances, some simplifications such as Prandtl number of 1.0 and the sinusoidal oscilation of the inlet Mach number with 2.5 percents of an amplitude of deviation, were assumed without loss of generality. The tip clearance effect and the viscosity term, the third term on the right hand side of (2), moreover, were omitted for the simplification of the computation. The control surface was fixed at the three chords axially ahead of the blade row and the pitchwise periodicity of the flowfield was furthermore assumed. Then the unsteady but uniform inlet condition was expected. One period of the sinusoidal oscillation consisted of 36 time increments. The final results with the 35 different Mach number distributions at the respective time increments were shown in Fig. 5. The envelopes of the different distributions are represented using the upper and the lower bounds of them. Now for the present run the control surface was assigned at the 0.2-axial-chord ahead of the rotor. Owing to the reference points on the control surface, the first approximation could be easily integrated into the run. The sinusoidal oscillation of the inlet deviation was matched to the rotor speed such that every sets of succeeding four blades met the similar inlet condition. After adding the omitted viscosity term to the first approximation[1], the unsteady inlet condition started from the one blade after another under the blade relative frame and then caused the non-uniformity as the whole.

For the transonic rotor flow the code was written in FORTRAN for a HITAC S3800/480 and it required a memory of about 600 Mega bites for the present non-uniform case, as working volume. The current run required approximately 1 hour of the additional CPU time. The stability in the computation was very good.

The results for the axial, pitchwise and radial Mach number maps on the cross-sectional surface selected at 0.1-axial-chord-downstream of the rotor were shown in Figs. 5 to 7, comparing to

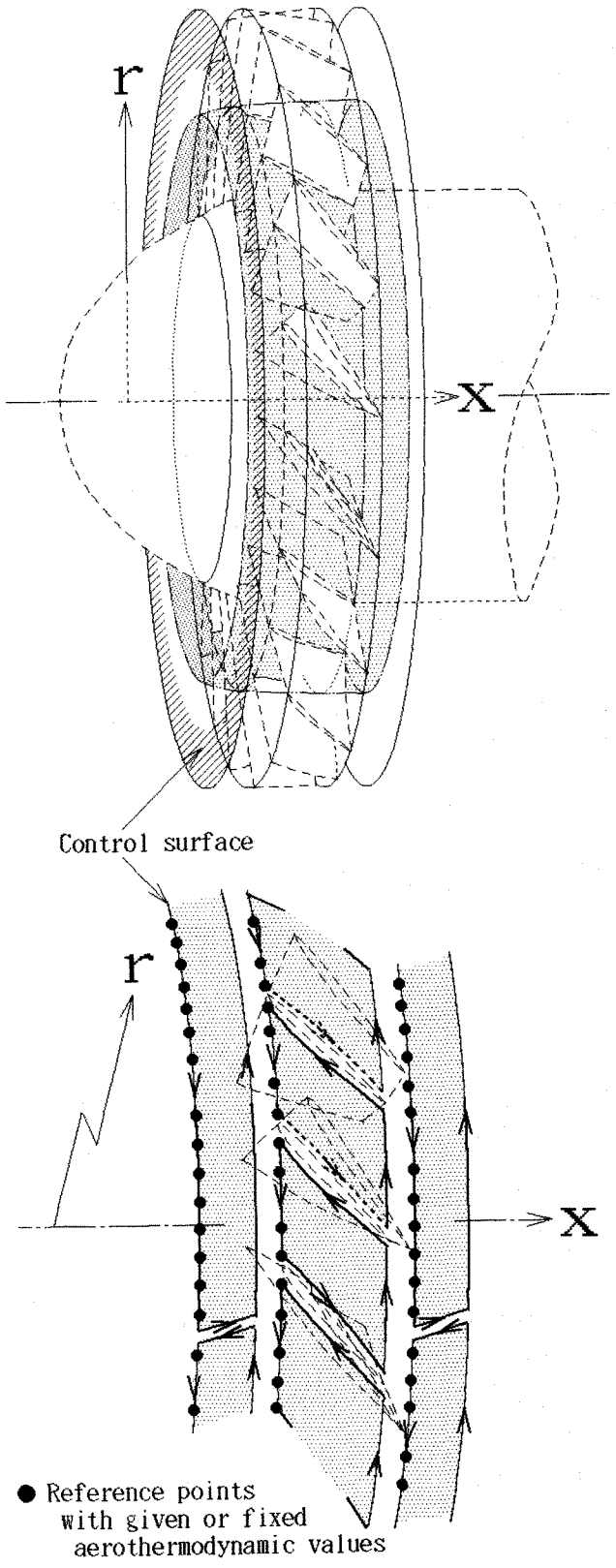

Fig. 3 Computation paths on a blade-to-blade surface

the first approximations, respectively. In the figures the abscissae are the blade passing periods and the ordinates the radial distance non-dimensionalized by the tip radius. The radii 0.700 and 0.950 stand for the respective locations near the hub and the blade tips. Fig. 5 shows the axial Mach number maps. The underestimated secondary flow effect in the previous result[1] in the outer half part of the annular flowfield was apparently improved. The obscure pitchwise periodicity observed in the experiment[6] was detected. The pitchwise non-uniformity in the map was apparently caused by the unsteadiness given at the upstream after the mutual interactions among the various flow conditions at the different time increments. Also the map suggests the possibility of the prediction of the secondary flows due to the unsteadiness. Figs. 6 and 7 illustrated the pitchwise and radial Mach number maps, respectively. These maps obviously showed the similar tendency for the axial ones. In Fig. 7, as for the radius ratio of 0.700, the results simply include the effect of the wall curvature of the hub. The radial maps characteristically surveyed the secondary flow phenomena. The current integral operator method can give the more detailed maps of the flow, but was used only for the comparison between the results.

Conclusion

For the approach to the numerical experiment of the arbitrary inlet conditions in the three-dimensional compressible viscous cascade flows, a numerical method based on the pseudo-analytic function theory for the initial boundary value problem is presented. A numerical example was shown to demonstrate an important role of the negligible order of unsteadiness detected at the inlet in the turbomachine performance. The code can give the stable numerical computations even for the flows with the unsteady inlet conditions and shows the applicability of the method to the future numerical experiments.

References

1. Miyazaki, T.,"Numerical Analysis of 3D Compressible Cascade Flows with Arbitrary Inlet Condition Using the Navier-Stokes Solver Based on Pseudo-analytic Functions ," Computational Fluid Dynamics Journal, Vol.3, No.2, July 1994.

2. ibid.,"A Theoretical Solution of the Unsteady Three-Dimensional Compressible Navier-Stokes Equation by Pseudo-analytic Function Theories : An Application to Arbitrary Turbomachines," Proc. of the 2nd Japan-Soviet Union Joint Symposium on Computational Fluid Dynamics, August 1990, Tsukuba, Japan, Vol. 1, 235-251.

3. Colton, D.L., Solution of Boundary Value Probblems by the Method of Integral Operators, Pitman Pub., 1976.

4. Vekua, I.N., Generalized Analytic Functions, Pergamon Press, London, 1962.

5. Kerrebrock, J.L.," The M.I.T. Blowdown Compressor Facility," MIT GTL Rep. 123, Sept. 1975.

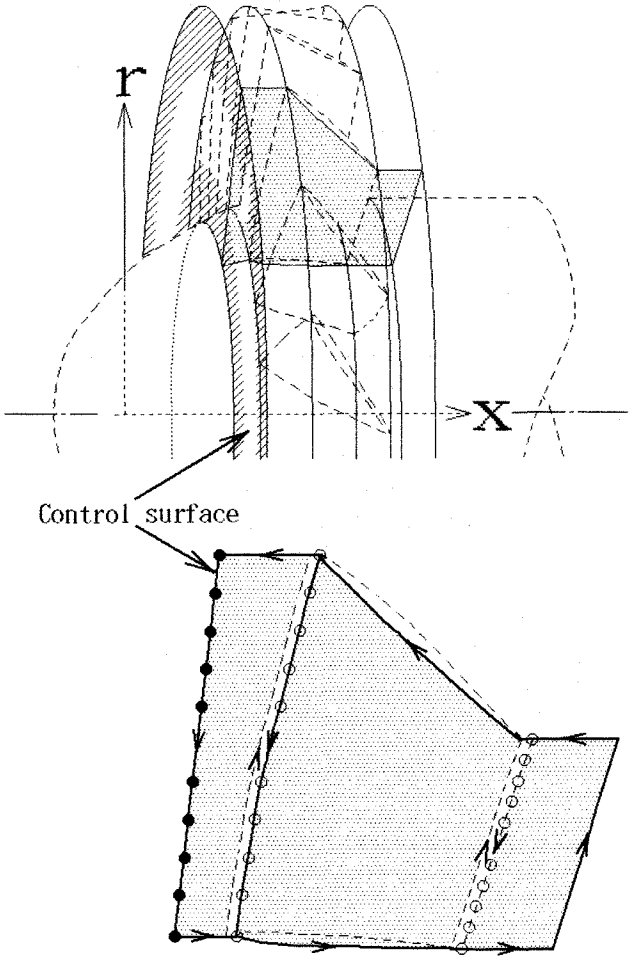

Fig. 4 Computation paths on a meridional surface

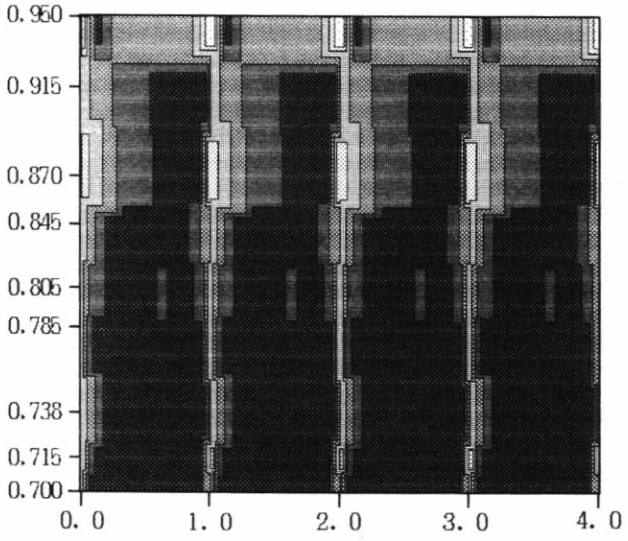

Upper bound[Ref. 1]

(a)

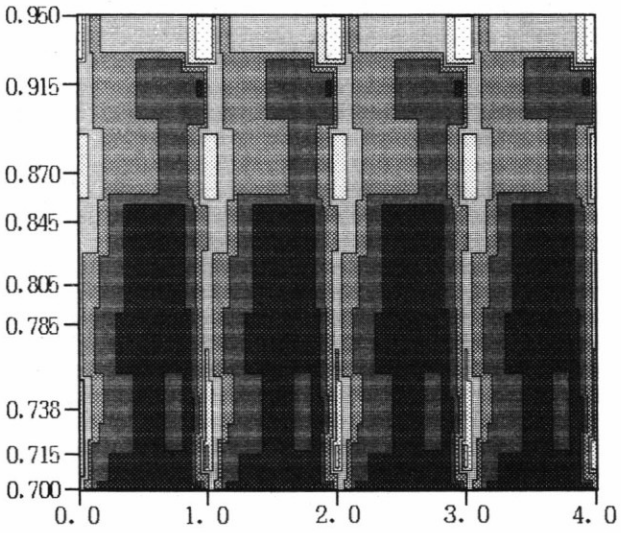

Lower bound[Ref. 1]

(b)

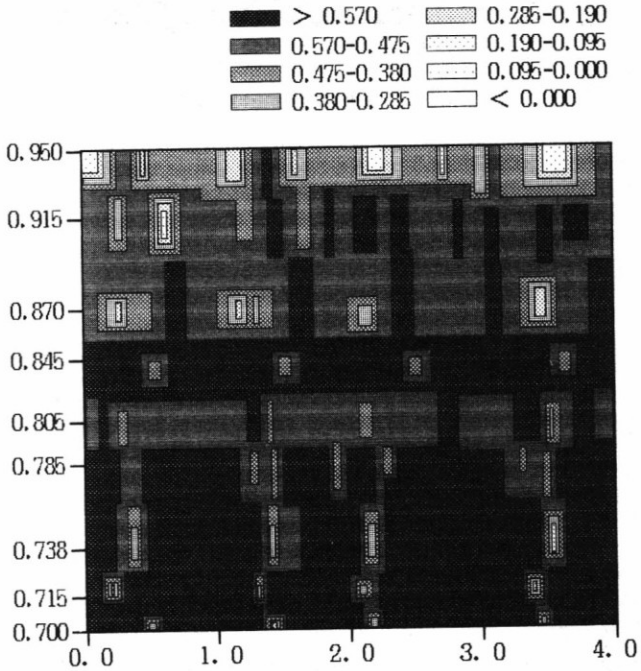

Non-uniformity caused by the unsteadiness

(c)

Fig. 5 Axial Mach number maps at 0.1-chord-downstream of rotor

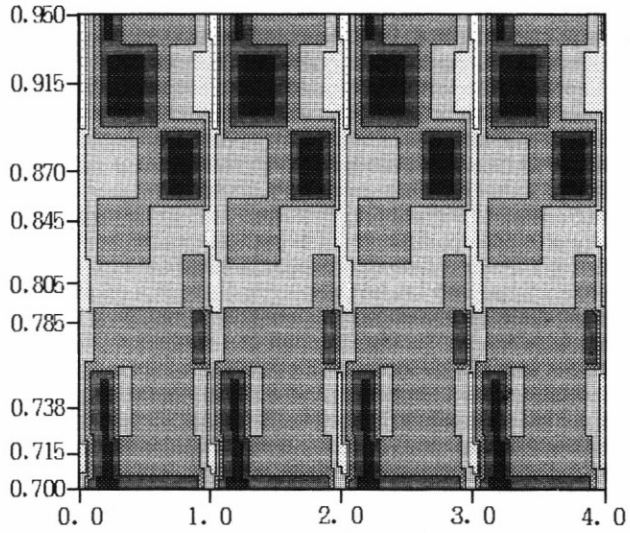

Upper bound[Ref. 1]

(a)

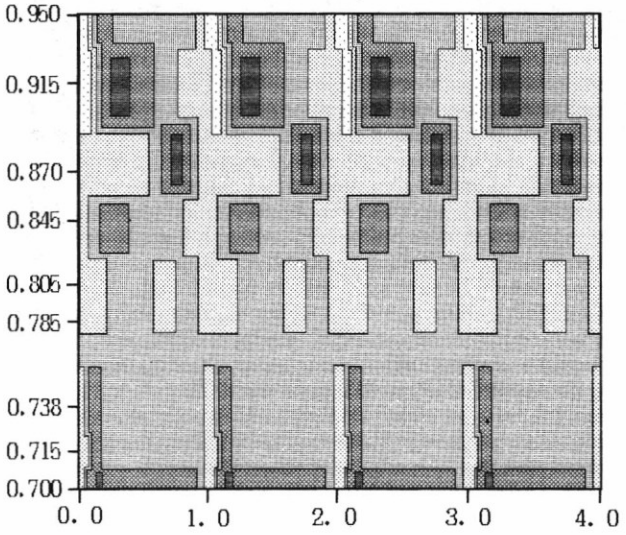

Lower bound[Ref. 1]

(b)

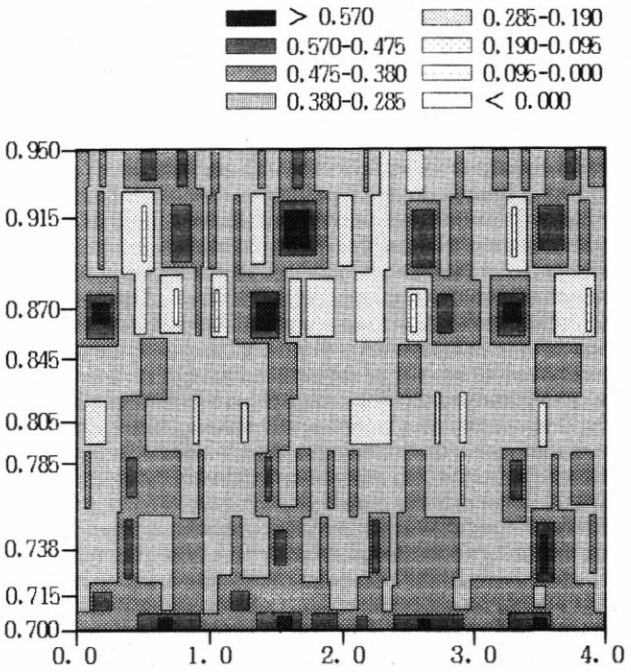

Non-uniformity caused
by the unsteadiness

(c)

Fig. 6 Pitchwise Mach number maps
at 0.1-chord-downstream of rotor

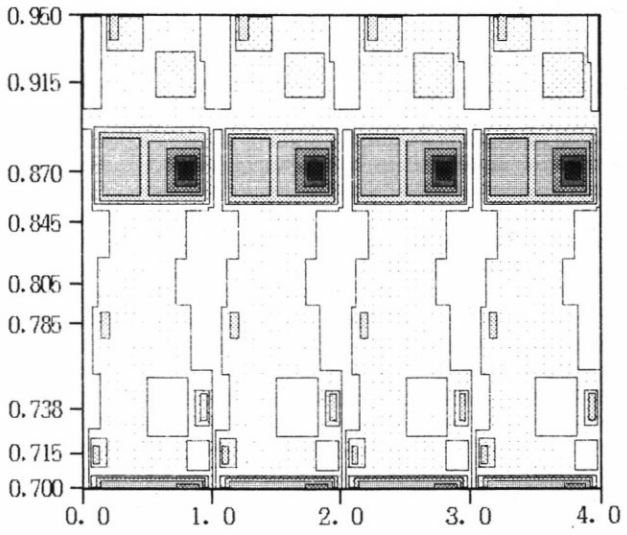

Upper bound[Ref. 1]

(a)

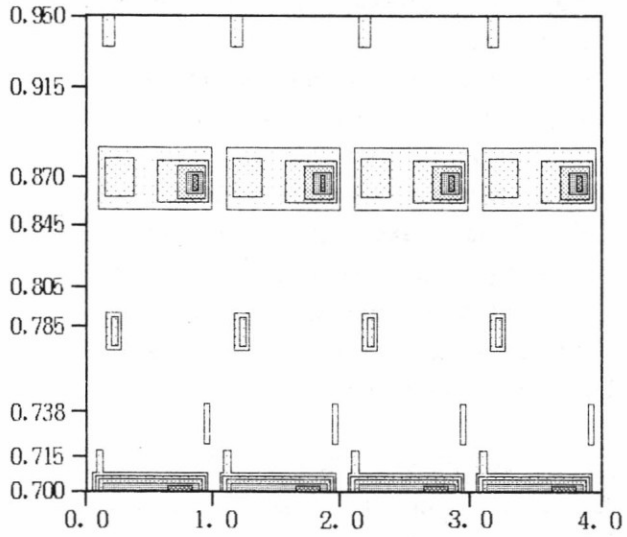

Lower bound[Ref. 1]

(b)

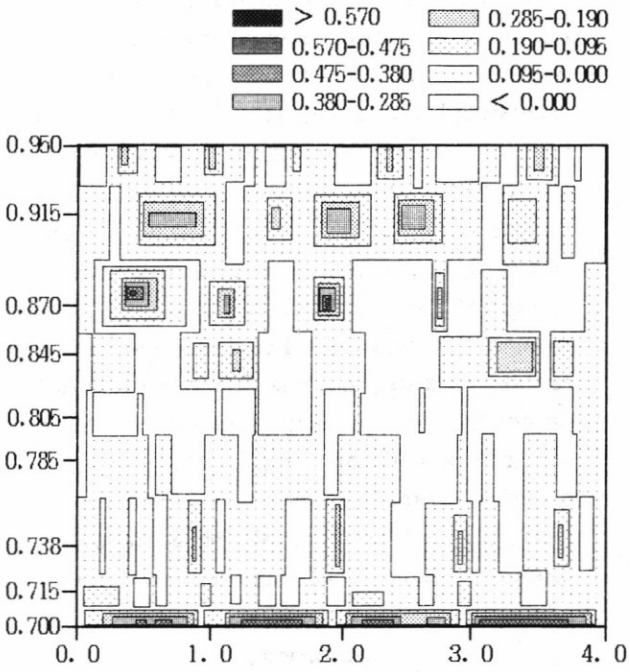

Non-uniformity caused
by the unsteadiness

(c)

Fig. 7 Radial Mach number maps
at 0.1-chord-downstream of rotor